Age determination of stellar populations

Tina Olsson

Lund Observatory
Lund University

Age determination of stellar populations

Bachelor's project report

Tina Olsson

Supervisor: Sofia Feltzing

Lund Observatory

31$^{\text{st}}$ August, 2012

Abstract

The formation history of the Milky Way galaxy is presently a subject of frequent investigation within astronomy. Of interest when constructing theories of the Galaxy's formation is the question of whether or not there exist any gradients regarding ages of the stars within the stellar disks.

In this project, a method for age-determination of stellar populations based on the Sobel Kernel edge detection technique has been utilised. The method has been tested on existing photometric data (obtained in the Strömgren photometric system) in order to find turn-off colours for samples of stars. The turn-offs were subsequently compared with isochrones to obtain the age of the youngest population within each sample. Evaluation of the method yielded that it could indeed be useful for age-determination when searching for gradients within the stellar disks of the Milky Way galaxy. Suggestions for improvements, additional tests and future applications of the method are presented. Also included are turn-off colours obtained for the samples; dependent on metallicity, Galactic longitude, distance from the Sun and height above the Galactic plane.

Populärvetenskaplig sammanfattning

Vintergatan, vårt hem i Universum, är den enda galax vi har möjlighet att studera i detalj. Med hjälp av observationer och beräkningar vet vi idag ungefär hur Vintergatan ser ut. Vi vet att Vintergatan består av en tunn skiva av stjärnor, stoft och gas, kallad den tunna disken. I mitten har den en utbuktning, kallad bulben. I och runtomkring finns en lite tjockare skiva med lägre densitet och bestående nästan enbart av stjärnor, kallad den tjocka disken. Det finns också en sfäriskt formad halo som är glesast av allt. Vi vet också att Galaxens skiva innehåller en struktur med spiralarmar. Detaljerna i Galaxens utseende, och framför allt hur den bildades, är dock fortfarande ett mysterium som dagens astronomer försöker lösa.

För att lösa detta mysterium måste vi studera stjärnorna i Vintergatans olika delar. Om vi kan undersöka huruvida stjärnorna i den tjocka disken till exempel är äldre än de i den tunna disken kan detta säga oss någonting om i vilken ordning diskarna bildades. Men vi vill också ta reda på om stjärnorna *inom* den tjocka disken skiljer sig åt i ålder. Då kan vi få ytterligare ledtrådar till hur Vintergatan skapades. Målet med detta arbete är att undersöka åldrar på grupper av stjärnor, kallade populationer, på olika höjd och riktning i Galaxen, för att se hur de skiljer sig åt och om det verkar finnas mönster.

Det är svårt att bestämma åldern för en enda stjärna, men det går att bestämma åldern för en population av stjärnor. När stjärnor åldras sväller de upp till röda jättar, och blir också svalare. Vi vet också att tunga stjärnor åldras snabbare än lätta. Eftersom de tunga stjärnorna från början är hetare än de lätta kommer det därför att efter en tid bli så att det inte finns några stjärnor som är varmare än en viss temperatur. Om vi därför lyckas mäta vilken temperatur de hetaste stjärnorna i en population har kan vi sedan ta reda på hur gamla stjärnorna är. Med den här metoden kan vi dock bara hitta den yngsta populationen i en grupp stjärnor.

Vår metod använde ett program skrivet i programmeringsspråket Python för att analysera mätvärden från observationer av stjärnor i olika riktningar i Vintergatan. Resultaten det gav stämmer överens med dagens teorier om hur Vintergatan ser ut, exempelvis att det finns yngre stjärnpopulationer in mot Galaxens mitt och nära skivan än ut mot kanterna och högre upp. Vi tror att metoden mycket väl kan vara användbar i sökandet efter åldersskillnader inom Galaxens diskar, men först behöver metoden testas på fler stjärnor och exaktheten bestämmas. Metoden kan just nu upptäcka skillnader i ålder, men inte bestämma den faktiska åldern av en särskild population.

Contents

1 Introduction

1.1 The Milky Way galaxy

1.1.1 Galactic structure

The Milky Way galaxy (see Fig. 1), our home in the Universe, is the only galaxy which we have the possibility of studying in detail. Faraway galaxies cannot be resolved highly enough to allow investigation of stellar populations within. While the details of the Milky Way's structure remains a subject of investigation even today, there now exists profound observational evidence regarding the overall structure of the Galaxy.

Figure 1: A 360-degree panorama of the Milky Way galaxy as seen from Earth. Image source: Wikimedia Commons.

The Milky Way is a barred spiral galaxy, with a diameter of 30 kpc (Schneider 2006). Two major spiral arms dominate the structure; the Scutum-Centaurus arm and the Perseus arm. Between these are a number of minor arms, one of which is called the Orion spur. Within this arm, at a distance of 8.5 pc from the Galactic centre, resides our sun.

It has been found that the Galaxy consists of four main components: the thin disc, the thick disk, the bulge, and the halo. The thin disk has a scale-height[1] of about 300 pc, and contains most of the stars in the Galaxy, as well as clouds of gas and dust. It is mainly here that formation of new stars take place, since the interstellar clouds provide the necessary material. The ages of stars belonging to the thin disk population range from newly formed stars to at least 8 Gyr (Covey et al. 2010).

---

[1]Scale-height denotes the distance from the Galactic plane at which the density has decreased a factor of e from the value at its centre. The scale-heights of the disks is still a matter of investigation. The values used here are approximate. Source: Schneider (2006).

A note on elemental abundances in stars: when the first stars formed, only hydrogen and helium was available as stellar material. During the lifetime of the stars, heavier elements (up to iron) were created through fusion. When the heaviest stars of the first generation died through supernova, these elements (and even heavier ones created in the explosion) were distributed into the interstellar gas. These metals[2] were later incorporated into the stars of following generations. Therefore metal abundance can be a crude indicator of the age of a star, where high Z correlates with young age.

There is a distinction between so-called population I stars, which are of Solar-like metallicity ($Z \sim 0.02$) and reside mainly in the thin disk, and population II stars. These are stars that are metal-poor ($Z \sim 0.001$), old (12-14 Gyr), and differs in position and velocity dispersion throughout the Galaxy from population I stars. The oldest population II stars reside in the halo. The halo has a scale-hight of around 3 kpc and is about 600 times more thinly populated than the thin disk. Globular clusters can be found within all components of the Galaxy, including the halo.

The thick disk has a scale-hight of circa 1 kpc, and consists mainly of intermediate-age population II stars (10-12 Gyr). These stars differ from the stars of the thick disk not only in metallicity and age, but also kinematically; rotating more slowly around the centre of the Galaxy. Lastly, there is also the Galactic bulge, located across the central region of the Galaxy and containing the Galactic bar. It has a scale-height of about 400 pc, and consists mainly of metal-rich intermediate-age population II stars.

1.1.2 Formation of the Galaxy

The details of the Galaxy's formation process remains a matter of investigation. There are two major theories of how the Milky Way could have formed. The *monolithic* collapse model assumes that the whole galaxy formed through a single collapse of gas in an area of higher-than-average density in the early universe. In this theory, the halo formed from the initial gas, and the gas settling down into a rotating disk commenced to form the thick and the thin disk from increasingly metal-enriched gas. Evidence for this theory is found through the consequently old ages of globular clusters found in the halo, and

---

[2]Throughout this work the astrophysical definition of metals is used: all elements heavier than helium. To denote the raw fraction of elements in the stars' composition, the letters X, Y and Z are used to represent hydrogen, helium and metals, respectively.

that a metallicity-gradient for stars correlating with Galactocentric distance has been detected within the Galaxy.

The *hierarchial* model, by contrast, assumes that stars first formed from small clouds, creating clusters and dwarf galaxies. These supposedly later agglomerated together to form the much larger Galaxy. Observational evidence supporting this theory include stellar streams in the halo resulting from in-falling dwarf galaxies.

These observations combined suggest that the formation history of the galaxy is more complicated than either one of these models by themselves. Recent theories have, in order to explain all observational evidence, suggested a scenario where the Milky Way formed in two stages: starting with a monolithic collapse of a proto-galactic cloud, and subsequently experiencing mergers of smaller galaxies (Schneider 2006). In order to confirm and inquire into the details of this scenario, it is important to study the galactic disks. Especially the presence or absence of gradients within the disks will be important clues as to their formation history. Through observations it has been confirmed that there exist a metallicity gradient (decreasing with increasing z^3), see e.g. Du et al. (2004). This could well be an effect of different densities and thus contributions from the thin disc, the thick disk, and the halo at different altitudes.

However, there is currently no consensus regarding whether or not there exist any metallicity gradients *within* the disks. The thick disk is especially of interest here. If it formed through gas collapsing into a thinner and thinner disk, it is expected that it would show a vertical metallicity gradient. If it, however, originates from a merger event where a dwarf galaxy collided with the thin disk of the Milky Way and kinetically perturbed it, one would expect to find that the thick disk is a combination of Galactic disk stars whose orbits got perturbed in the merging event and stars having originally formed in the incoming dwarf galaxy.

While the quest for metallicity gradients presently is a subject of frequent investigation (e.g. Siegel et al. 2009), few studies have been made with the motif to search for age gradients. In this project, a method for age-determination of stellar populations is presented, applied on a set of photometric data in order to look for gradients within the stellar disks, and finally the benefits and shortcomings of the method utilised are discussed.

---

[3]z denotes height above the Galactic plane.

1.2 Strömgren photometry

The data used in this study were obtained through observations in the Strömgren photometric system. In Strömgren photometry, four filters u, v, b and y are used to collect light at different wavelengths during the observations (see Fig. 2). The y filter is centred at 550 nm, and can thus be
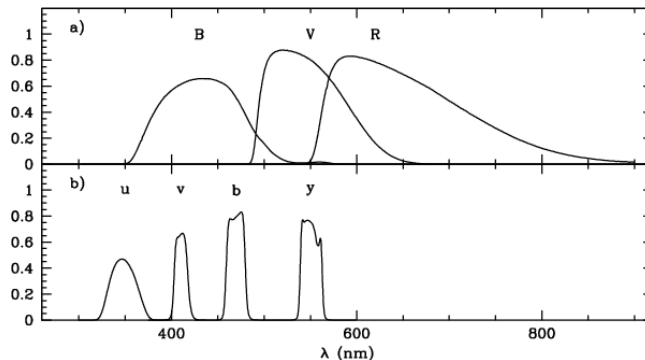

Figure 2: Throughput as a function of wavelength for each filter in **a)** the conventional Johnson photometric system, and **b)** the Strömgren photometric system. Figure from Árnadóttir et al. (2010).

used interchangeably with the V filter of the Johnson photometric system (Strömgren 1963). It has a half-width of 20 nm. The b filter is centred at 470 nm with a half-width of 10 nm. It thus encompasses the Hβ absorption line, but no other strong absorption lines. $(b - y)$ measures the steepness of the stellar spectral energy distributions, and is therefore a good colour-, and hence, temperature indicator. The higher the value of a star in the $(b - y)$ index, the redder and cooler it is. Since throughout this work only de-reddened photometric data have been used, y and $(b - y)$ will henceforth represent y_0 and $(b - y)_0$ (respectively), for convenience.

The v filter is located at 410 nm with a half-width of 20 nm. It is thus centred on the Hδ, and also encompasses many other absorption lines. Therefore, it is very metallicity-sensitive. The u filter is centred at 350 nm with a half width of 38 nm. It is located blue-wards of the Balmer jump, so combined with the v filter the size of this discontinuity can be measured. The u filter is also metallicity-sensitive: it is affected by line blanketing (reduction of light due to absorption lines) about twice as much as the v filter is.

Combining all filters, the following distance-independent photometric in-

4

dices can be constructed:

$$m_1 = (v - b) - (b - y)$$
$$c_1 = (u - v) - (v - b).$$

The m_1 index is metallicity-sensitive, and allows for photometric metallicity determinations (without the need for spectroscopy) to good accuracy. For a detailed discussion of the metallicity determinations and calibrations of the data used in this study, see Árnadóttir et al. (2010). The term *metallicity* will henceforth throughout this work be taken to mean photometrically determined metallicity, and be denoted by [Fe/H] (even though incorporating all metals, not just iron, nota bene). It is a logarithmic quantity denoting metal abundance, and in general values in this index for stars range from about -5 to 0.5 dex (Gray 2005).

The c_1 index measures the Balmer jump, and is thus luminosity-sensitive. This index is designed not to be very metallicity-sensitive, and can therefore be used to separate dwarf stars from giants without getting stuck in a metallicity-luminosity degeneracy. This is done in Árnadóttir et al. (2010) for our data, leaving only dwarf stars to be used in this study.

Among the advantages of Strömgren photometry is the fact that distance-independent metallicity measurements can be performed for a large number of stars simultaneously, without the need of medium-resolution spectroscopy. Among the drawbacks is that since the filters are narrow, the exposure times in order to collect enough light are very long, leading to a great sensitivity to observational circumstances.

1.3   Age determination through isochrones

As stars evolve they follow a distinctive path in the colour-magnitude diagram (CMD). They start off on the main sequence and after a time, growing larger (which increases their luminosity) and redder, move on to the red giant branch (RGB). The time it takes for a star to evolve onto the RGB is dependent on its initial mass; heavier stars evolve more quickly than light ones. If one plots stars of all masses in a CMD at a certain point in time, one will obtain a pattern where there are no stars which are bluer than a certain value. This value is called the turn-off colour (TO), and such a collection of stars is called an isochrone. An example of isochrones can be seen in Fig. 3. An isochrone is strictly speaking a theoretical construction, based on theories

of star formation and stellar evolution. Simulated isochrones are then calibrated against observational data, making them (as plotted and used here) a semi-empirical entity.
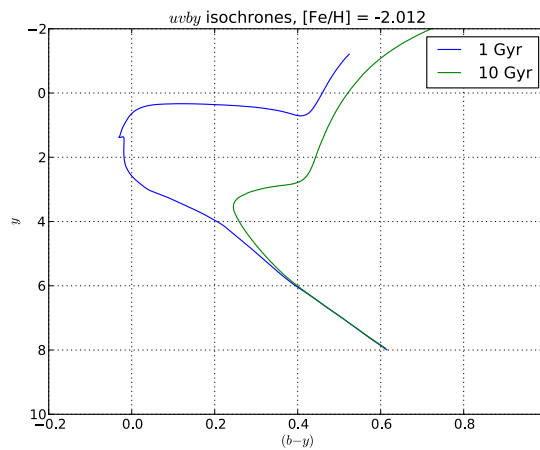
(a) Isochrones of low metallicity, plotted in the Strömgren photometric system.
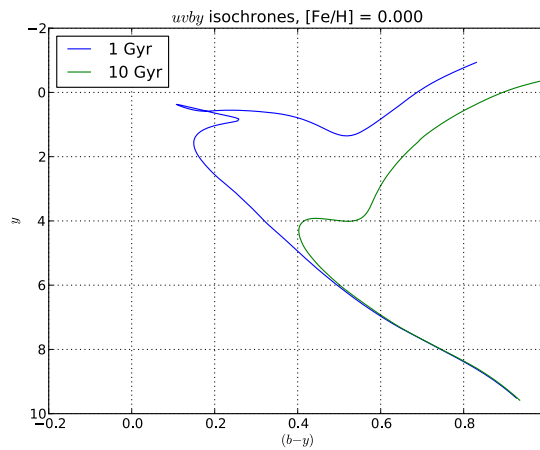
(b) Isochrones of high metallicity, plotted in the Strömgren photometric system.

Figure 3: Isochrones of ages 1 and 10 Gyr for stars of (a) low metallicity, and (b) high metallicity.

The turn-off age of a star is not determined by its initial mass alone, but

also by its metallicity. Increased metallicity affects the lifetime of a star by means of increasing its opacity. Greater opacity causes higher temperature, which in turn leads to the star burning its fuel more rapidly, thus moving off the main sequence earlier than a star of equal mass but with lower metallicity would do. Increased metallicity also has the effect of altering the stars' spectra. Especially iron absorbs more light in the blue part of the spectrum than in the red, which leads to a line blanketing effect through which the stars appear redder. All these effects change the appearance of the isochrones, as can be seen when comparing the metal-rich isochrones in Fig. 3(b) with the metal-poor ones in Fig. 3(a). Paying attention to the scale on the abscissa when comparing the two plots, it can be noted that increased metallicity leads to a redder turn-off colour. Evidently, there exists a metallicity-age degeneracy; it is impossible to determine the age and metallicity of a single star simultaneously.

If, however, the metallicity is known for a single population of stars, isochrones can be used to determine the age of that stellar population. The idea is then to find beyond which value of the colour index used (e.g. $(b - y)$ in the Strömgren photometric system) there are no bluer stars. This value is compared with isochrones of the same metallicity as the population, and the age of the population is concluded to be that of the isochrone with corresponding TO colour. This method is commonly applied to stellar clusters, both globular and open ones (see e.g. Chaboyer 2001). However, if the population is not mono-age and mono-abundance, as is the assumption in stellar clusters, then the detected TO colour could be misleading. Populations of different ages could have TOs close enough to each other that the detected TO of the youngest population really is a superposition of TOs of populations of different metallicities. In that case, synthetic CMDs must be constructed and compared with the data, and re-modelled until the situation reflects observations (see e.g. Pasetto et al. 2012). This is however not explored in this work.

2 Method

2.1 The data sets

The data used for analysis in this project is photometric data obtained in the Strömgren *uvby* system, using the Isaac Newton Telescope and the Wide

7

Field Camera. Included are 3521 stars identified as dwarfs, with metallicity determinations based on the photometry and stellar distances determined using stellar isochrones and photometry from the Sloan Digital Sky Survey (SDSS, see e.g. Abazajian et al. 2003). Observations, dwarf identifications, metallicity calibrations, de-reddening and distance determinations were carried out by Árnadóttir et al. (2010). The observed star-fields lie along the lines of sight towards the dwarf spheroid galaxies Hercules, Draco, Ursa Major II and Sextans. The directions of the different lines of sight with respect to the Milky Way are shown in Fig. 4. Towards Draco are two lines of sight, differing by 0.8 degrees on the sky, denoted by Draco 0 and Draco B. The number of stars in each observed field can be found in Table 1.
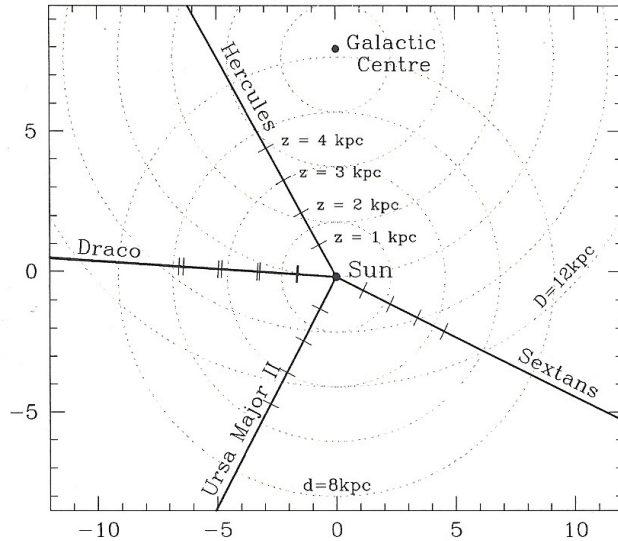

Figure 4: Schematic picture looking down on the Galactic plane. The directions of observation are shown in solid lines. The dotted circles mark distance in the Galactic plane from the Galactic centre (D) and from the sun (d). The tick-marks on the solid lines represent height above the Galactic plane (scale shown towards Hercules). Note that there are two fields of observation towards Draco, differing somewhat in height above the Galactic plane. Figure from Árnadóttir (2009).

All observational fields were also covered by SDSS, and all stars observed in *uvby* were also found by SDSS. The observed stars in all directions lie in

8

magnitude range $15.0 < y < 18.5$, the completeness[4] being over 91 % in this magnitude range. Notably, in the brighter magnitudes the completeness is very close to 100 %. In the directions towards Draco B and Hercules are also included stars in the magnitude range $18.5 < y < 20.0$ with completeness ranging from 90 % to 67 % towards Draco B and from 93 % to 83 % towards Hercules. For a further discussion of the data and its completeness, see Árnadóttir et al. (2010). Unless otherwise specified, only stars within magnitude range $15.0 < y < 18.5$ were used in the present analysis.

Table 1: The number of stars in each field of observation from Anna Árnadóttir's observations. The total number of stars is 3521.

Direction of obs.	# of stars
Draco 0	379
$(15.0 < y < 18.5)$	
Draco B	354
$(15.0 < y < 18.5)$	
Draco B	634
$(18.5 < y < 20.0)$	
Hercules	599
$(15.0 < y < 18.5)$	
Hercules	1090
$(18.5 < y < 20.0)$	
Sextans	233
$(15.0 < y < 18.5)$	
Ursa Major II	239
$(15.0 < y < 18.5)$	

The metallicities as a function of the colour index $(b - y)$ for each population are shown in Figure 5. In the plots it is clearly evident that beyond a certain value of $(b - y)$ there are no bluer stars. This sharp edge is the TO of interest in this study, which correlates with the age of the youngest population in the sample. In the plots it is worth noting that the TO colour does not appear to be the same for stars of different metallicities; there could

---

[4]The completeness was calculated as the ratio of detected number of stars in the *uvby* observations compared with detected number of stars in the SDSS.

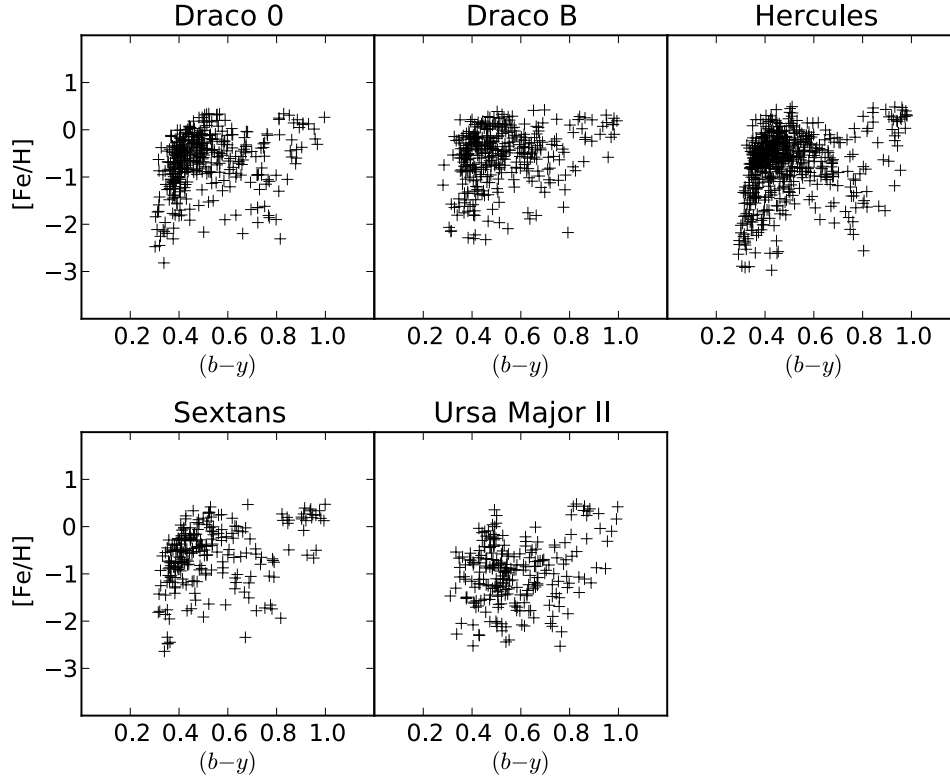be a trend where stars of higher metallicity have a redder TO colour. This is what we investigate.

Figure 5: Metallicity plotted versus colour index $(b - y)$ for stars in each direction (error bars not included). Note that beyond a certain value of $(b - y)$ there are no bluer stars: this is the TO of the youngest population in the sample.

Figure 6 shows a histogram of observational errors for $(b - y)$ for all stars. It can be noted that all errors are below 0.05 mag. The stars with errors between 0.04 and 0.05 mag all belong to the fields in the directions of Hercules and Ursa Major II, while all stars belonging to the fields towards Draco and Sextans have errors between 0.01 and 0.02 mag. This is an effect of different weather conditions on the nights of observation of the respective fields, which resulted in shallower data for the Hercules and Ursa Major II
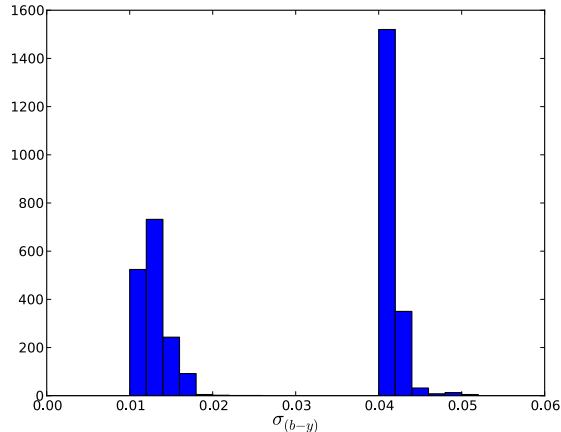
10

fields.

Figure 6: Histogram of the errors in $(b-y)$ for stars in all fields.

A histogram of the errors in [Fe/H] of all data is shown in Fig. 7. Evidently, most errors are smaller than 0.5 dex, so 0.5 dex can justifiably be set as bin size when dividing stars with respect to metallicity. Unfortunately there was no time to experiment with different bin sizes, so it is difficult to say how large the problem of stars jumping between bins would have been. It should be pointed out that most of the errors larger than 0.5 dex belong to stars in the magnitude range $(18.5 < y < 20.0)$. This is to be expected, since fainter magnitudes inevitably lead to larger uncertainties in the data obtained.

A histogram of distances to stars in all directions can be seen in Fig. 8. As can be seen, most stars lie within 400 pc of the Sun, which limits the possibilities of investigating age differences as a function of galactic longitude. A bin size of 200 pc was however chosen, with all stars further away than 1 kpc were grouped into one bin. This last bin is in general poorly populated.

A histogram of height above the Galactic plane of stars in all directions is shown in Fig. 9. As can be seen, most of the stars lie within $0 < z < 300$ pc, and thus the majority of them are expected to belong to the thin disk. Unfortunately, this limits the possibilities of investigating the thick disk, especially at higher altitudes. Nevertheless, a bin size of 100 pc was chosen, with all stars of $z > 1$ kpc (very few) grouped into a single bin.
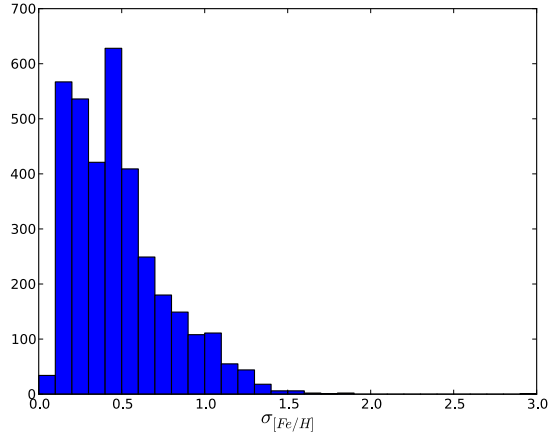
11

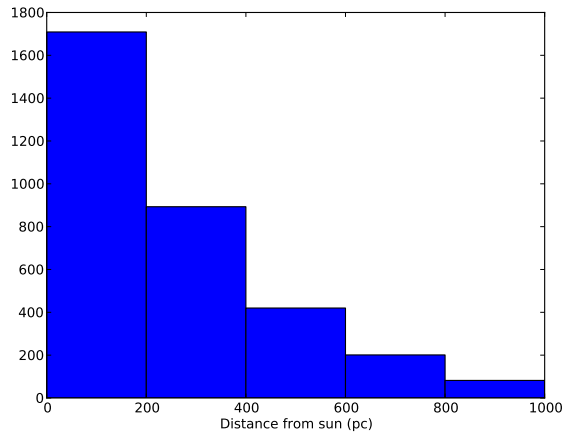Figure 7: Histogram of the errors in [Fe/H] for stars in all fields.

Figure 8: Histogram of line-of-sight distances to stars in all fields. There are also stars located in the distance range $1000 < d < 20000$ pc. They are, however, very few, and have been omitted from the picture for clarity.

2.2   Analysis procedure

In order to find the TO colour for each sample in a mathematically well-defined way (rather than estimating by hand) a standard image-processing edge-detection technique called Sobel Kernel was used in a similar way as in
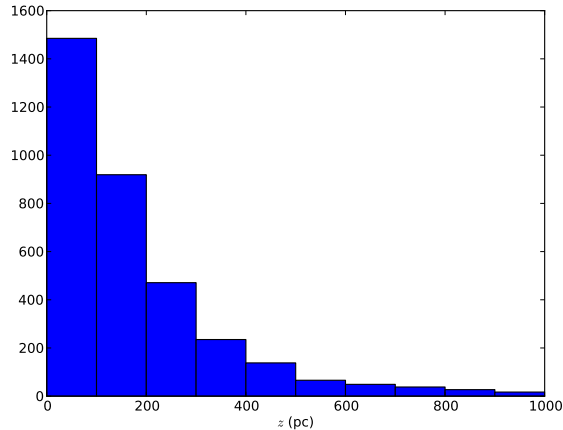
Figure 9: Histogram of height above the Galactic plane (z) for stars in all fields. There are also stars located in the range $1000 < z < 4000$ pc. They are, however, very few, and have been omitted from the picture for clarity.

Tabur et al. (2009) and Jofré & Weiss (2011). Here it was implemented in a program written in the Python programming language. (The initial routine was written by Daniel Adén for another purpose and modified and extended by me to detect TO colours. The code is available in Appendix A.)

In the Sobel Kernel method, the distribution of $(b-y)$ values for a sample of stars is modeled by a continuous probability distribution, defined as follows:

$$\Phi((b-y)) = \sum_{i=0}^{N} \frac{1}{\sqrt{2\pi}\sigma_i} \exp\left[-\frac{((b-y)-(b-y)_i)^2}{2\sigma_i^2}\right], \qquad (1)$$

where $(b-y)_i$ and σ_i are values of the colour index and their uncertainties, respectively, for each star. N is the total number of stars in the sample. The inclusion of σ_i means that the measurement errors in the data are accounted for. This corresponds to assuming that each star can be represented by a Gaussian probability distribution, its width depending on the uncertainty in the measurement of the $(b-y)$ value. These distributions are summed to become one continuous probability distribution. An edge-detection filter is then applied to the distribution function. It has the following form:

$$E((b-y)) = \Phi((b-y) - \Delta(b-y)) - \Phi((b-y) + \Delta(b-y)), \qquad (2)$$

13

where $\Delta(b-y)$ represents a step size which can be specified. Throughout this work the step size was set to 0.01. The filter response corresponds to the difference between two consecutive values of the probability distribution function. The value of $(b-y)$ for which the filter response yields the smallest value (i.e. the largest absolute value; since the slope of the distribution curve is positive the smallest value will be negative) is then returned as the TO colour. This corresponds to the point in the distribution function where its slope is at its steepest. Figure 10 shows an example of the application of the method to our data.
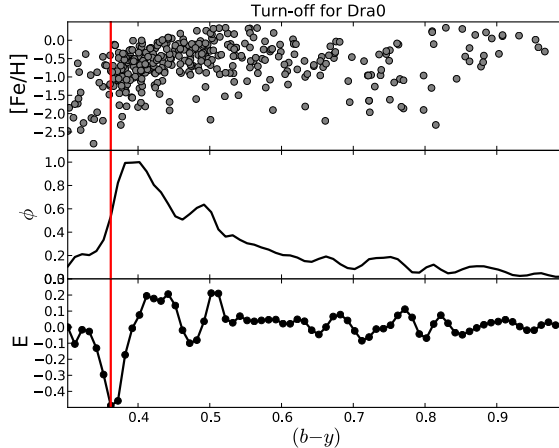

Figure 10: Turn-off colour detected (using the Sobel Kernel edge detection method) for all stars along the line of sight towards Draco 0. In the uppermost panel, every star in the sample is plotted in an [Fe/H] versus colour diagram. In the middle panel, the total probability distribution Φ (Eq. (1)) of the stars in the sample is plotted. In the lowermost panel, the filter response E (Eq. (2)) is plotted, and its largest absolute value is marked with a vertical line, which consequently also marks the steepest point of the probability distribution function, and in turn also marks the turn-off colour of the stellar population.

By dividing the data into bins of different metallicities, a metallicity-dependent TO colour could be obtained for each sample of stars. Since most errors in the metallicity are smaller than 0.5 dex (see Fig. 7), the bin size was set to 0.5 dex. Three bins were chosen between [Fe/H] $= -1.5$

14

and [Fe/H] = 0, with two additional open bins containing all stars with [Fe/H] > 0 and [Fe/H] < −1.5 respectively, making in total five bins.

The five TO colours (obtained using the Sobel Kernel method) for each sample were consequently plotted in a [Fe/H] versus $(b - y)$ plot, together with lines indicating age, in this case 8 and 14 Gyr. The lines used are based on the isochrones of VandenBerg et al. (2006). This type of plot, i.e. bringing TO colours together with isochrones in this fashion was first implemented in von Hippel & Bothun (1993). An example of such a plot can be seen in Fig. 11. For illustrative purposes, all stars used in each analysis are included in the plots (without error bars for clarity). Thus the plot also include stars that are redder than the TO. These stars may be main-sequence stars or sub-giant. As noted in § 2.1, any potential background (or otherwise) RGB stars have already been discarded from the sample (Árnadóttir et al. 2010).
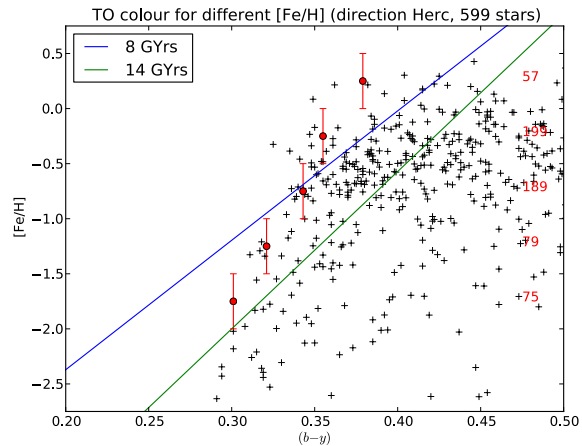

Figure 11: TO colour for different metallicities of stars in the direction of Hercules. The diagonal lines represent isochrones. The vertical lines on the TO points marks the metallicity bins. Note that these are *not* error bars, and that the red dot does *not* mark the average of the stellar distribution, only the centre of each bin (except for the uppermost and lowermost bins). The numbers on the right denote the number of stars in each bin. Also note that the uppermost and lowermost metallicity bins really includes all stars of metallicity above [Fe/H] = 0 and below [Fe/H] = −1.5, respectively, though not depicted as such.

15

2.3 Data analysis

2.3.1 Metallicity dependencies

As a first test, the data in each field were run through the Sobel Kernel edge-detection program, and the obtained TO points were plotted together with isochrones. The results are shown in Fig. 11 to Fig. 14.
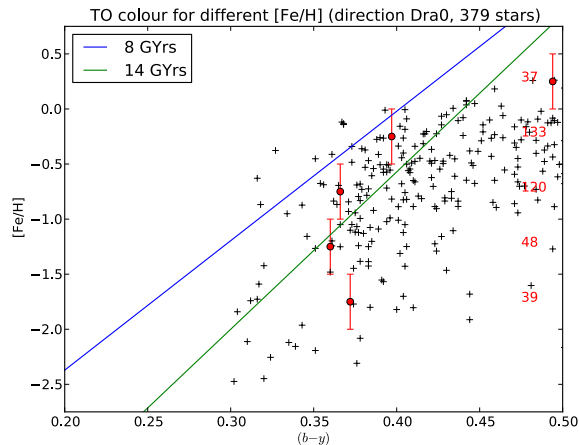

Figure 12: TO colour for different metallicities of stars in the direction of Draco 0.

In the Hercules sample (Fig. 11), there appears to be a trend where more metal-rich stars are younger than the more metal-poor ones. Stars with [Fe/H] > -0.5 seem to include populations younger than 8 Gyr, while the more metal-poor stars have no population younger than 8 Gyr.

In the two Draco samples (Fig. 12 and Fig. 13) some peculiarities can be seen. Some of the TO points lie below the 14 Gyr isochrone, indicating that they would contain no population younger than the age of the Universe. These reason for these strange results is likely that there are too few stars in the sample (in particular, too few TO stars). To improve on the number statistics, the two Draco samples were added together for further analysis. The Sextans sample show similar peculiarities, probably resulting from too few stars. It was also combined with the Draco sample, since their directions both point out towards the edge of the Galaxy (see Fig. 4).

Combining the two Draco samples yielded the plot in Fig. 15. Although there are still some peculiarities in the lower metallicity bins, it can now be
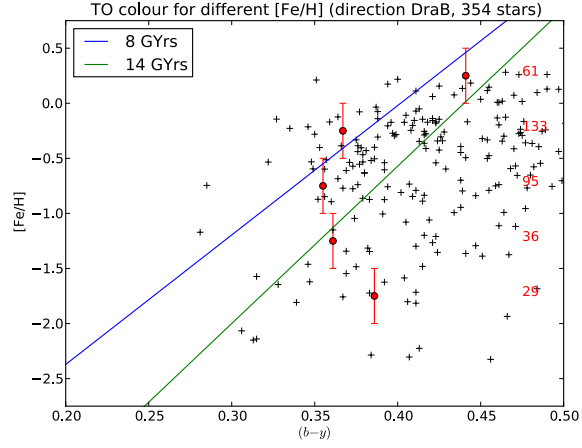
16

Figure 13: TO colour for different metallicities of stars in the direction of Draco B.
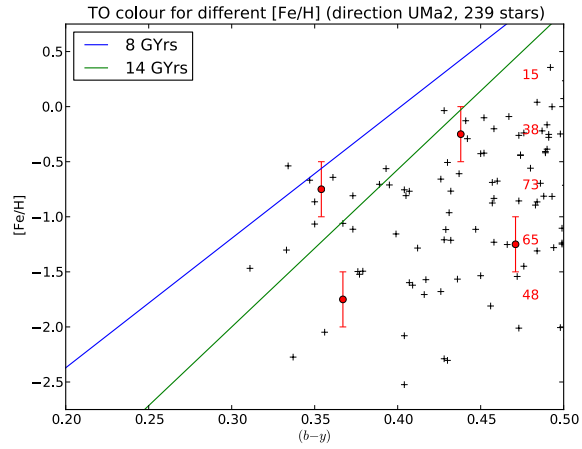

Figure 14: TO colour for different metallicities of stars in the direction of Ursa Major II.

concluded that the sample contain no populations younger than 8 Gyr. There could be a trend where more metal-poor stars belong to an older population.

Combining the Draco samples with the Sextans sample yielded the plot in Fig. 16. It shows similar results as the Draco samples alone, but with less
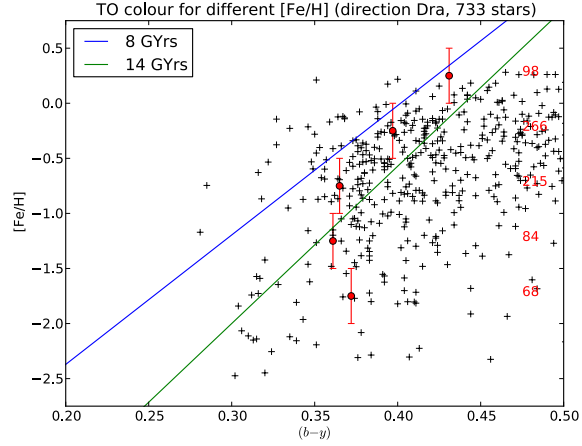
Figure 15: TO colour for different metallicities of stars in the direction of Draco.

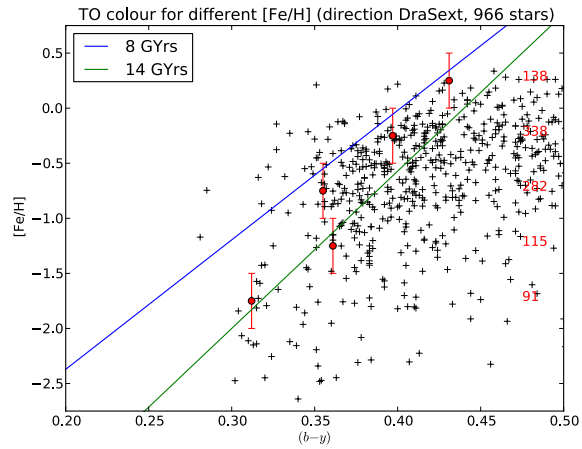fluctuations in the lower metallicity bins.

Figure 16: TO colour for different metallicities of stars in the directions of Draco and Sextans.

The Ursa Major II sample (Fig. 14), however, showed such bad results that the sample was discarded from further analysis. The reasons for the bad quality of the sample are probably few stars and large photometric errors in

the observations.

2.3.2 Distance dependencies

The next step in the analysis was an attempt to investigate whether there exist a dependency of population age as a function of distance from the sun. The samples were divided into distance bins of size 200 pc between 0 and 1000 pc, plus an additional bin including all stars further away than 1000 pc. The analysis, however, proved limited by the small number of stars in each bin for large distances.

For the Hercules sample, only the first two bins could be investigated. These results are shown in Fig. 17 and Fig. 18. It is difficult to draw any conclusions concerning distance dependence from these two plots. Possibly the closer bin could contain a younger population among the more metal-rich stars than the bin further away, but it is difficult to say whether it is a real effect or an artefact arising from the fact that the number of stars in certain bins are low.
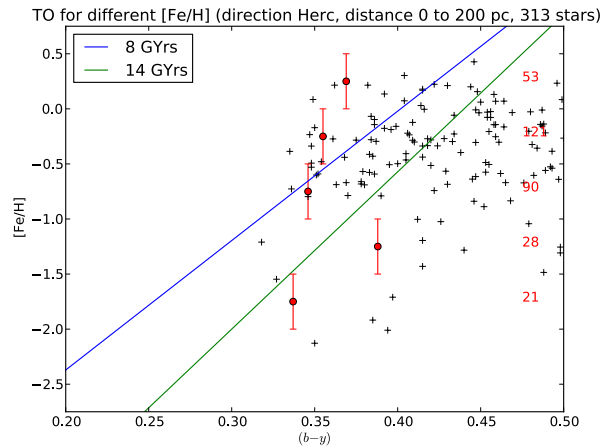

Figure 17: TO colour for different metallicities of stars in the direction of Hercules, distance 0 to 200 pc.

For the Draco sample, the closest three bins contained sufficiently many stars for the analysis to be feasible, but the number of stars in each metallicity bin was still so low that the plots yielded no intelligible results.
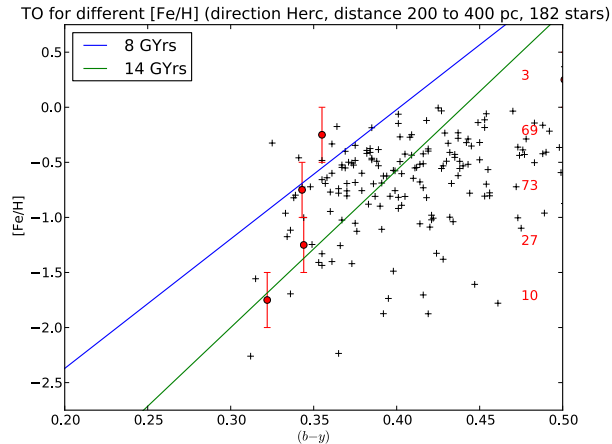
Figure 18: TO colour for different metallicities of stars in the direction of Hercules, distance 200 to 400 pc.

For the combined Draco and Sextans sample, the analysis could be performed on the three closest bins, and yielded the plots in Fig. 21 to Fig. 23. Despite the reasonably large number of stars (472) in the closest bin, the plot in Fig. 21 suggests that in almost all metallicity bins, there is no population younger than 14 Gyr. What is the reason for this unreasonable result?

It is found that the reason for this behaviour is related to the magnitude cut of the observations. Stars with the same intrinsic brightness located close to us appear brighter than those further away. Thus the stars differ in apparent magnitude, the values increasing with distance[5]. Recalling that the observed stars should show an isochrone-like pattern with a TO, it can be imagined that these structures are displaced vertically in a CMD when sorted with respect to distance. Thus if the magnitude cut is made to only encompass stars fainter than a certain value (in this case 15.0 mag) there is a risk that the TO stars at the closer distances are emitted (being too bright), and only stars further down the main sequence are included. The situation is visualised schematically in Fig. 19.

This would in turn result in the program detecting a far too red TO colour. By looking at the plot in Fig. 20, where $(b - y)$ is plotted versus distance for all stars used in the analysis, it can clearly be seen that this

---

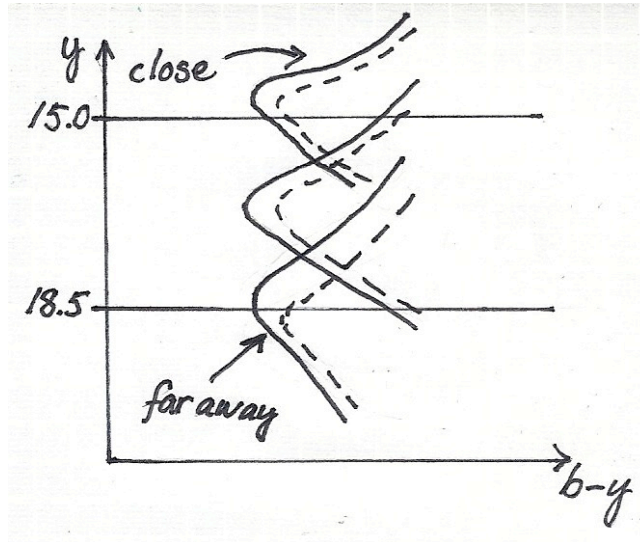[5]Recall that large magnitudes corresponds to faint stars!

Figure 19: The magnitude cut effect illustrated. The figure shows a schematic picture of stars in a CMD. The vertically displaced isochrone-like curves represent stellar populations located at different distances from the Sun. The dashed curves represent stars at the same distances, but with higher metallicities. The horizontal lines represents the magnitude cut of the observations, the window of observation lying between the two lines. Here it is evident that close-by TO stars are lost in the observations, instead we see only stars further down the main sequence.

magnitude-cut effect has indeed affected the data. There is clearly evident a gap at close distances where blue stars are missing.

Distances between 200 and 600 pc show similar effects (see Fig. 22 to 23), though not as severe. In this case, however, the magnitude-cut effect should not be a big problem (according to Fig. 20). In this case it is probably the small number of stars in most metallicity bins, especially in the TO-region, which gives rise to strange effects. It could possibly be concluded that there exist no populations younger than 8 Gyr within the investigated distances, but the significance of this result is low.

2.3.3 Dependencies on height above the Galactic plane

Next, we investigated whether age changes as a function of height above the Galactic plane, i.e. whether any vertical age gradients appears to exist. The
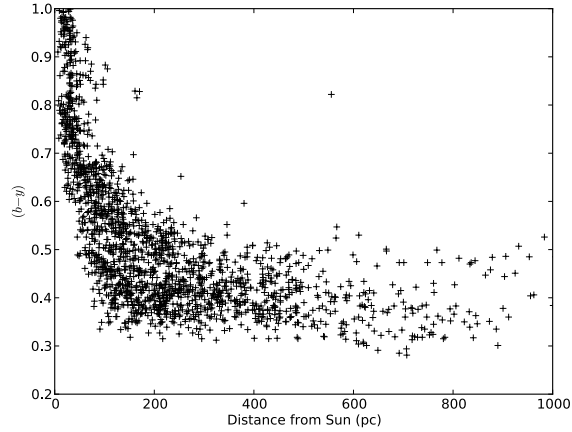
21

Figure 20: $(b - y)$ for all stars, plotted versus distance from the Sun. Note that close-by blue stars are missing due to the magnitude cut, the stars being too bright. It can also be noted that red stars are missing at large distances, these stars in contrast being too faint. This is however not a problem since only TO stars are of interest in this study.
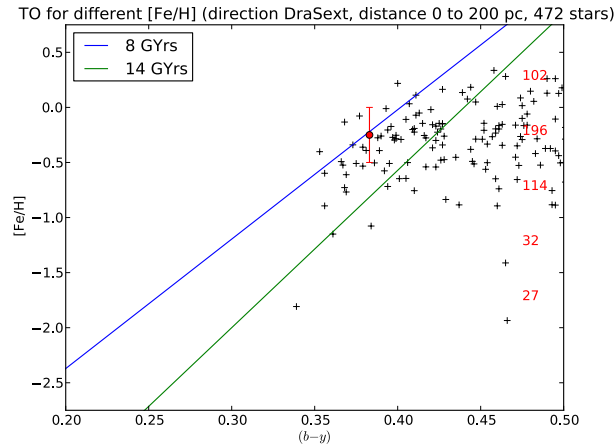

Figure 21: TO colour for different metallicities of stars in the directions of Draco and Sextans, distance 0 to 200 pc. Note that most detected TO colours are redder than 0.5 dex, and thus not visible in the plot.

22
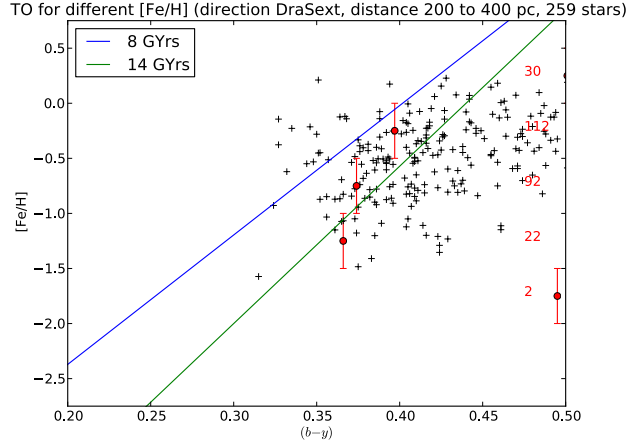
Figure 22: TO colour for different metallicities of stars in the directions of Draco and Sextans, distance 200 to 400 pc.
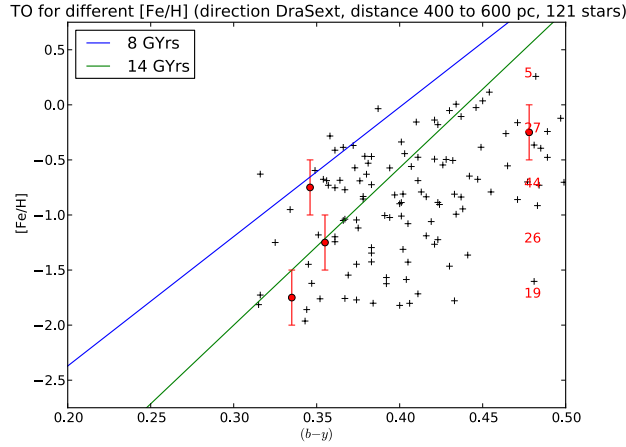
Figure 23: TO colour for different metallicities of stars in the directions of Draco and Sextans, distance 400 to 600 pc.

data of each field was divided into bins of size 100 pc between 0 and 1000 pc above the Galactic plane, with an additional bin including all stars higher up than 1000 pc. This in total made eleven bins.

Since the bins with large z in each sample were very scarcely populated, the data in magnitude range $18.5 < y < 20.0$ were also included, which

increased the number of stars somewhat. However, they were still too few to make analysis possible for bins of z over 400 pc, even if all stars of z greater than 400 pc were added together. Thus the aim of investigating the higher altitudes of the thick disk was not feasible to pursue here. The results obtained where analysis was possible were however the following.

For Hercules, see Fig. 24 to Fig. 27. The bin closest to the galactic plane show similar peculiarities (extremely red TO colours) as discussed in § 2.3.2. Also in this case the abnormalities are assumed to derive from the magnitude-cut effect; that turn-off stars are missing from the data at z close to the galactic plane.

Figure 24: TO colour for different metallicities of stars in the direction of Hercules, height above Galactic plane 0 to 100 pc.

Regarding the bins of higher z, apart from an extremely red TO for the bin of highest metallicity in the 200 to 300 pc z bin, there appears to be a trend of older populations with greater z. Between 100 and 200 pc there are populations (of high metallicity) younger than 8 Gyr, but higher up essentially all populations appear to be older than 8 Gyr.

For Draco and Sextans, analysis could only be made for bins of z of 0 to 300 pc. The results are shown in Fig. 28 to Fig. 30. In the z bin closest to the galactic plane the TO colours are unreasonably red, most likely due to TO stars missing due to magnitude cut here as well. What could possibly be derived from the other plots is that there appears to be no populations younger than 8 Gyr close to the galactic plane within these samples. It is
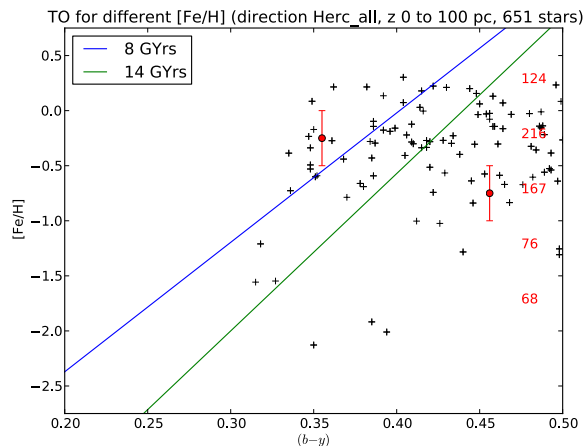
Figure 25: TO colour for different metallicities of stars in the direction of Hercules, height above Galactic plane 100 to 200 pc.

Figure 26: TO colour for different metallicities of stars in the direction of Hercules, height above Galactic plane 200 to 300 pc.

however difficult to obtain a detailed picture, since some of the metallicity bins contain few stars, particularly very few TO stars.
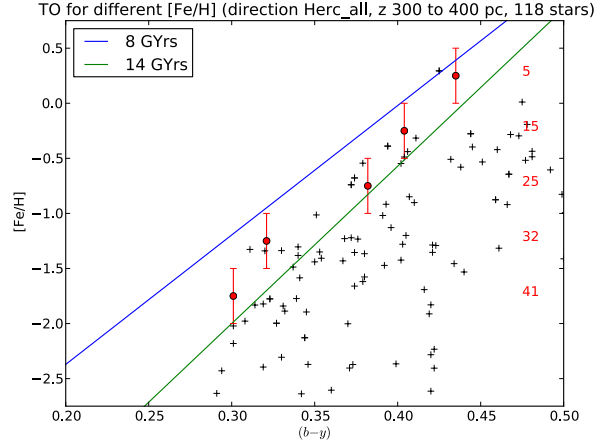
Figure 27: TO colour for different metallicities of stars in the direction of Hercules, height above Galactic plane 300 to 400 pc.
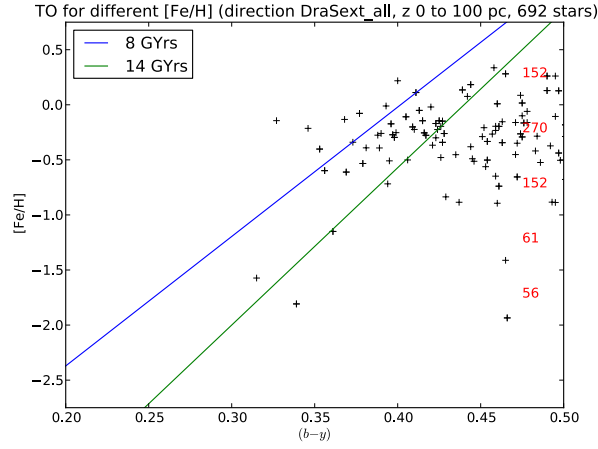
Figure 28: TO colour for different metallicities of stars in the directions of Draco and Sextans, height above Galactic plane 0 to 100 pc.

3 Discussion

3.1 Results

Regarding stellar age gradients with respect to direction in the galactic plane, the results obtained indicate that younger populations exist towards the
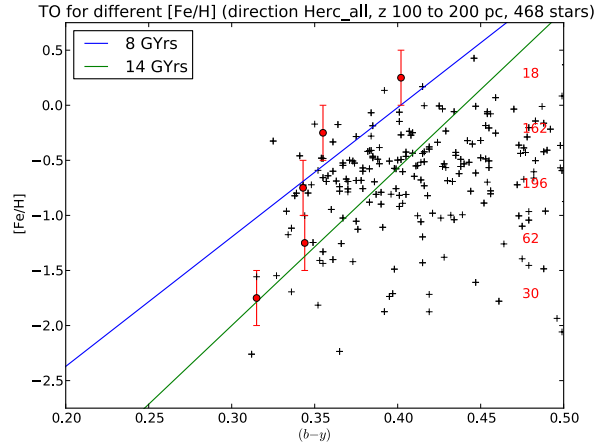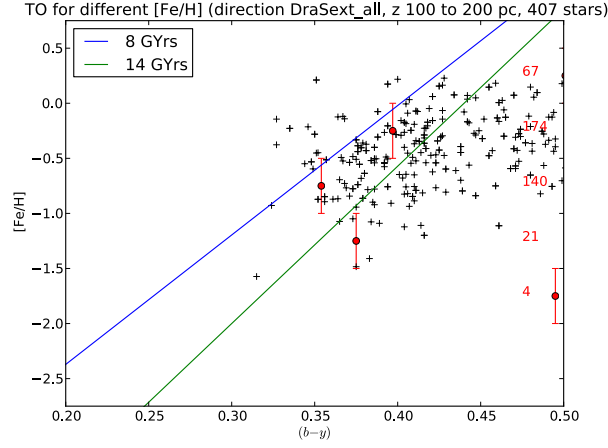
Figure 29: TO colour for different metallicities of stars in the directions of Draco and Sextans, height above Galactic plane 100 to 200 pc.
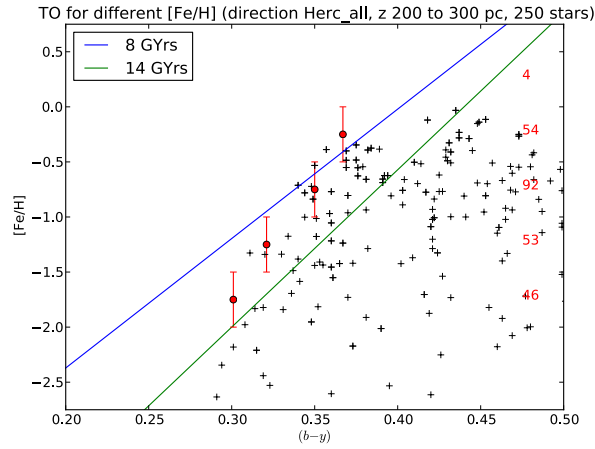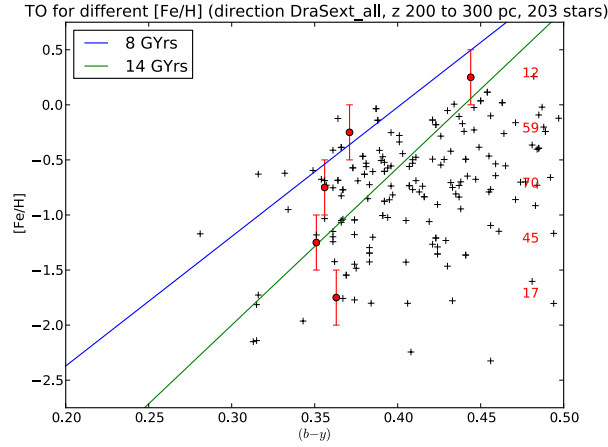

Figure 30: TO colour for different metallicities of stars in the directions of Draco and Sextans, height above Galactic plane 200 to 300 pc.

Galactic centre (towards Hercules) than towards the outskirts of the Milky Way. The analysis indicate that there are populations younger than 8 Gyr in the direction towards the Galactic centre, while all populations located outwards from the Sun are all older than 8 Gyr. This largely agrees with current understanding of Galactic structure; star formation is more frequent

in the central regions of the Galaxy than towards the edges, at least when considering regions close to the galactic plane (which most stars investigated in this study belong to).

The results of this study also suggest that younger populations exist among stars of high metallicity than for stars of lower metallicity. This is consistent with current understanding of Galactic chemical evolution.

Regarding gradients with respect to distance from the sun and height above the galactic plane no investigation could be done at distances further away than 600 pc and at z above 400 pc, due to the data being too sparse beyond these distances and altitudes. Thus the initial aim of investigating vertical gradients within the disks could not be pursued within the data sets available. As explained in § 2.3.2, the closest bins could not yield any useful results because of TO stars missing as a result of the magnitude cut. As for the bins left for investigation, indications could possibly be inferred towards younger ages of populations closer to the Sun and the Galactic plane, respectively. This is in accordance with current theories of Galactic structure.

Although the discussion of results throughout this work has focused on interpretation of plotted data, the numerical values of TO colours for all analyses run were also documented. These will not be investigated in this study, but can be found for future reference in Appendix B.

3.2 Limitations of the data sets

Had more time been available for this study, further testing and evaluation of the age-determination method could have been made. Firstly, a more extensive data set would have been needed in order to investigate age-gradients within the thick disk and higher altitudes of the thin disk, as was the initial aim of the project. A limitation of the method is that it cannot be run without stars in all metallicity bins. An additional requirement is naturally that TO stars need to be included (consider as an example Fig. 14 where the data clearly is insufficient for application of the method). Therefore it is important to know the completeness of the samples used, and also an awereness of whether or not any significant stars are lost through the magnitude cut. A possible candidate for data to test the method on could be samples from SDSS, more specifically from SEGUE[6] which has spectroscopically determined metallicities for its stars. For studies of age gradients within the

---

[6]Sloan Extension for Galactic Understanding and Exploration

disks, it would be practical to only use stars astrometrically determined to kinematically belong to e.g. the thick disk. While it is not feasible to separate populations with respect to kinematics without any overlap it could still be interesting to apply the method on such samples.

One peculiarity of the data is that blue stars of high metallicity appear to be missing from the samples (see Fig. 5), which would account for the fluctuations in the uppermost metallicity bin. This is likely to be an effect of the magnitude cut (discussed in § 2.3.2), where TO stars of high metallicity located far away might have fallen away due to being too faint.

3.3 Evaluation of method and suggestions for future work

Although the data used in this study proved to be too sparse for detailed investigations, the method in general have shown reasonable results where it could be applied. One important aspect to consider before attempting to use it for detailed age-determination is the resolution of the technique, both concerning metallicity and colour. The metallicity bin size was throughout this work set to 0.5 dex (with two open bins). This could be argued to be justifiable when considering the errors in the metallicity measurements, but it could also be interesting to experiment with different bin sizes, perhaps located differently, to see what effects this would have on the results.

It could also be of interest to apply a running mean, or a so-called *fiducial sequence*, instead of fixed metallicity bins. As a test, this was done for the Hercules sample (see Fig. 31). In the test, the bin size was kept at 0.5 dex, while the separation between the bins (step size) was set to 0.03. In this way, each star could belong to several metallicity bins, and an idea of how sensitive the method is to different metallicity binning could be obtained. Comparing with the result obtained when using separate bins (Fig. 11) the same behaviour can be observed here; where there appears to exist populations younger than 8 Gyr for stars with [Fe/H] $>\sim -0.5$, while the more metal-poor ones appear to belong to an older population. There is however a trend of stars around -0.5 lining up nicely along the 8 Gyr isochrone which can not be observed in the previous test. It could be that this way of binning yields more details in the age measurements.

Had more time been available, this would have been investigated on more samples in order to confirm this conclusion. Further inquiry into the matter
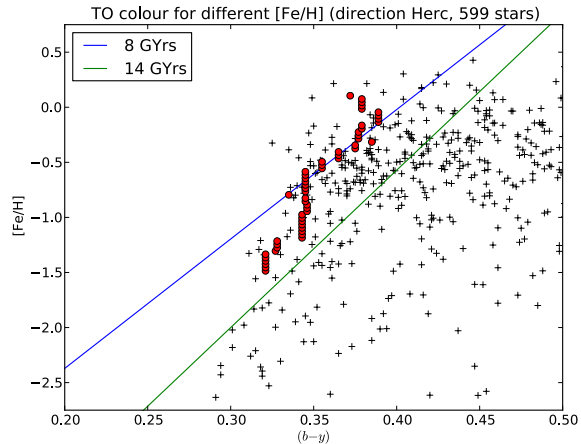
Figure 31: Fiducial sequence of TO colours for all stars in direction towards Hercules (compare with Fig. 11). Each dot represents the TO of one metallicity bin. The step size used is 0.03 dex, with a bin size of 0.5 dex.

could be done by changing the bin size and the step size and see how this affects the results. It is however important to keep in mind that the bin size cannot be made smaller than that there are stars in each bin, and should not be made much smaller than the errors in the metallicity measurement. With more exactly determined metallicities this could be possible, but such exact metallicity measurements are difficult to accomplish through photometry.

Using fiducial sequences, it would appear to be useful to compare with more isochrones. There is however also the issue of errors in $(b - y)$. The program, as it is constructed, yields no estimation of errors in $(b - y)$ of the TO colours found, therefore none have been plotted. These uncertainties are dependent on colour uncertainties of the individual stars, therefore a general uncertainty of the method cannot be set ad hoc, but have to be calculated in a well-defined way. This could be done through the boot-strap method used by Tabur et al. (2009) and Jofré & Weiss (2011). However, as this is beyond the scope of this study, the uncertainties of the TO colours obtained is left unaccounted for here. What could be said as a ballpark estimation is that since all errors in $(b - y)$ are smaller than 0.05 mag in the data sets used here the uncertainties should at least not be much greater than that. An uncertainty of 0.05 mag would however translate to a quite large uncertainty with respect to ages, so a well-defined calculation of the errors would be

essential in evaluating the exactness in age-determination of this method.

Thus detailed results regarding the specific ages of various populations are not feasible to obtain through our method, even if isochrones of more ages than 8 Gyr and 14 Gyr would have been used to compare with, since the errors in $(b - y)$ are unknown and the uncertainties in [Fe/H] have not been thoroughly investigated. In its current form, the method is qualitative rather than quantitative, showing relative ages of different populations but not being able to exactly determine the age of a specific population.

An additional aspect which could be interesting to investigate is TO colours measured in the $(v - y)$ colour index. Throughout this work all plots have been made with respect to $(b - y)$, but TOs have been calculated in this index as well (see Appendix B). The $(v - y)$ index is more metallicity-sensitive than $(b - y)$, which could possibly lead to a higher resolution in colour-space. It is however also possible that it would lead to a metallicity-colour degeneracy. This would have to be considered when applying the method in this colour index, but this as well is beyond the scope of the current study.

In conclusion, the method to determine the TO colour for the youngest stars and thus the age of these stars presented in this work is, after some adjustments and further testing, likely to be useful in the quest for age gradients within the stellar disks of our Galaxy. However, it will be difficult to enhance its resolution to the point of making it possible to detect whether the obtained TO is in fact a combination of closely-lying TOs of several different populations. Ideally, it should therefore be combined with CMD modelling, because it is on its own only able to detect the youngest population within a given sample.

Acknowledgements

References

Abazajian, K., Adelman-McCarthy, J. K., Agüeros, M. A., et al. 2003, AJ, 126, 2081

Árnadóttir, A. S. 2009, PhD thesis, ISBN 978-91-628-7922-8

Árnadóttir, A. S., Feltzing, S., & Lundström, I. 2010, VizieR Online Data Catalog, 352, 19040

Árnadóttir, A. S., Feltzing, S., & Lundström, I. 2010, A&A, 521, A40

Chaboyer, B. 2001, in Astronomical Society of the Pacific Conference Series, Vol. 245, Astrophysical Ages and Times Scales, ed. T. von Hippel, C. Simpson, & N. Manset, 162

Covey, K. A., Beers, T. C., Bochanski, J. J., et al. 2010, Measuring Stellar Ages & the History of the Milky Way (Astro 2010 white paper)

Du, C.-h., Zhou, X., Ma, J., et al. 2004, AJ, 128, 2265

Gray, C. D. F. 2005, The Observation and Analysis of Stellar Photospheres, 3rd edn. (The Edinburgh Building, Cambridge CB2 8RU, UK: Cambridge University Press)

Jofré, P. & Weiss, A. 2011, A&A, 533, A59

Pasetto, S., Chiosi, C., & Kawata, D. 2012, ArXiv e-prints

Schneider, P. 2006, Extragalactic Astronomy and Cosmology: An Introduction, 1st edn. (Springer-Verlag Berlin Heidelberg)

Siegel, M. H., Karataş, Y., & Reid, I. N. 2009, MNRAS, 395, 1569

Strömgren, B. 1963, QJRAS, 4, 8

Tabur, V., Kiss, L. L., & Bedding, T. R. 2009, ApJ, 703, L72

VandenBerg, D. A., Bergbusch, P. A., & Dowler, P. D. 2006, ApJS, 162, 375

von Hippel, T. & Bothun, G. D. 1993, ApJ, 407, 115

A Sobel Kernel Python code

```python
def tofinder(pop,minby=0,maxby=1.5,mineby=0,maxeby=1,\
minFeH=-4,maxFeH=2,mindist=0,maxdist=20000,\
minHAP=0,maxHAP=4000):
    """
    tofinder runs the Sobel Kernel edge-detection on metallicity-versus-
    colour plots of stellar populations. The data needs to be stored
    in a text file with the name 'pop_dist.txt', containing by,eby,m1,
    em1,FeH,eFeH,dist,HAP in columns 17,18,19,20,23,25,38,40,
    where pop is the name of the population.

    Parameters
    ----------
    pop : name of population, given as a text string (e.g. 'Dra0')
    minby : minimum value of b-y to include in computation
    (default is 0)
    maxby : maximum value of b-y to include in computation
    (default is 1.5)
    mineby : minimum value of error in b-y to include in computation
    (default is 0)
    maxeby : maximum value of error in b-y to include in computation
    (default is 1)
    minFeH : minimum value of [Fe/H] to include in computation
    (default is -4)
    maxFeH : maximum value of [Fe/H] to include in computation
    (default is 2)
    mindist : minimum value of distance (in parsec) to include
    in computation (default is 0)
    maxdist : maximum value of distance (in parsec) to include
    in computation (default is 20000)
    minHAP : minimum value of height above galactic plane (in pc)
    to include in computation (default is 0)
    maxHAP : maximum value of height above galactic plane (in pc)
    to include in computation (default is 4000)
    The default values are set to include all stars in all samples,
    i.e. leaving the data unfiltered.
```

```
Returns
-------
TOby : the turn-off colour in the b-y index
TOvy : the turn-off colour in the v-y index
nstars : number of stars taken into account in the computation
(after filtration)
by : a list of all (b-y) values used in the computation
FeH : a list of all [Fe/H] values used in the computation

Running the function on a distribution also returns two plots
with metallicity of each star, the total distribution (where each
data point is assumed to be Gaussian) and the filter response
plotted versus b-y and v-y, respectively. The detected edge
(TO) is marked in the plot.
"""
filename = '{}_dist.txt'.format(pop)
by,eby,m1,em1,FeH,eFeH,dist,HAP = loadtxt(filename,unpack=True,\
 usecols=[17,18,19,20,23,25,38,40])


#  Calculating the (v-y) index
vy = m1 + 2*by


#  Calculating the error in (v-y)
evy = sqrt(em1**2 + 4*eby**2)


#  A function to unzip zipped arrays
unzip = lambda l:tuple(zip(*l))


#  Creating a list containing the b-y values, their errors,
#  [Fe/H], v-y and their errors in tuples
list = zip(by,eby,FeH,vy,evy,dist,HAP)


#  A filter to remove stars values outside a desired interval
#  from the sample. a is by, b is eby, c is FeH, d is vy, e is evy,
#  f is dist, g is HAP.
filtby = lambda (a,b,c,d,e,f,g): minby < a < maxby
list = filter(filtby, list)
filteby = lambda (a,b,c,d,e,f,g): mineby < b < maxeby
```

```python
list = filter(filteby, list)
filtFeH = lambda (a,b,c,d,e,f,g): minFeH < c < maxFeH
list = filter(filtFeH, list)
filtdist = lambda (a,b,c,d,e,f,g): mindist < f < maxdist
list = filter(filtdist, list)
filtHAP = lambda (a,b,c,d,e,f,g): minHAP < g < maxHAP
list = filter(filtHAP, list)

(a,b,c,d,e,f,g) = unzip(list)
by = array(a)
eby = array(b)
FeH = array(c)
vy = array(d)
evy = array(e)
dist = array(f)
HAP = array(g)

#  Number of stars left in sample after filtering
nstars = len(by)

def sobel(data_x,data_y,err,res=0.01,pl=1):
    close('all')
    maxd=max(data_x) ; mind=min(data_x)
    xx=arange(mind,maxd,res)
    fi=zeros([len(xx)])
    for i in xrange(len(xx)):
        fi[i]=sum(1./(sqrt(2*pi)*err)*exp(-(xx[i]-data_x)**2/(2*err**2)))
    fi=fi/max(fi)
    E=zeros([len(xx)])
    for i in xrange(1,len(xx)-1):
        E[i]=fi[i-1]-fi[i+1]
    mi=xx[find(E==min(E))]
    if pl==1:
        figure()
        subplots_adjust(hspace=0.001)
        subplot(3,1,1)
        yticks(arange(-2.5, 0.5, 0.5))
        xlim(mind,maxd) ; ylabel(r'[Fe/H]',fontsize=18)
```

```
        plot(data_x,data_y,'o',color='grey')
        axvline(x=mi,linewidth=3, color='k')
        title('Turn-off for {}'.format(pop))
        subplot(3,1,2)
        xlim(mind,maxd) ; ylim(0., 1.1), ylabel(r'$\phi$',fontsize=18)
        plot(xx,fi,lw=3,color='k')
        axvline(x=mi,linewidth=3, color='k')
        subplot(3,1,3)
        yticks(arange(-.1, 1., 0.1))
        xlim(mind,maxd); xlabel(r'${\rm \by_0}$',fontsize=18)
        ylabel('E',fontsize=18), ylim(-0.2,0.2)
        plot(xx,E,'-o',color='k',lw=3)
        axvline(x=mi,linewidth=3, color='k')
        savefig('tofinder.pdf')
        show()
    return mi
TOby, TOvy = sobel(by,FeH,eby)[0],sobel(vy,FeH,evy)[0]
print 'Turn-off colour in b-y: {}'.format(TOby)
print 'Turn-off colour in v-y: {}'.format(TOvy)
print 'Number of stars in sample: {}'.format(nstars)
return TOby,TOvy,nstars,by,FeH
```

B Tables of TO colours

Table 2: Metallicity-dependent TO colour for dwarf stars along different lines of sight.

Direction of line of sight	[Fe/H]	# of stars (in bin)	TO $(b-y)$	TO $(v-y)$
Draco 0	> 0	37	0.494	2.312
	$0 - -0.5$	133	0.397	0.893
	$-0.5 - -1.0$	120	0.366	0.847
	$-1.0 - -1.5$	48	0.360	0.814
	< -1.5	39	0.372	0.663
Draco B	> 0	61	0.441	2.315
	$0 - -0.5$	133	0.367	0.989
	$-0.5 - -1.0$	95	0.355	0.825
	$-1.0 - -1.5$	36	0.361	0.819
	< -1.5	29	0.386	0.806
Hercules	> 0	57	0.379	2.267
	$0 - -0.5$	199	0.355	0.850
	$-0.5 - -1.0$	189	0.343	0.781
	$-1.0 - -1.5$	79	0.321	0.731
	< -1.5	75	0.301	0.634
Sextans	> 0	40	0.507	2.323
	$0 - -0.5$	72	0.392	0.976
	$-0.5 - -1.0$	67	0.354	0.819
	$-1.0 - -1.5$	31	0.348	0.808
	< -1.5	23	0.335	0.708
Ursa Major II	> 0	15	0.804	2.256
	$0 - -0.5$	38	0.438	1.068
	$-0.5 - -1.0$	73	0.354	0.820
	$-1.0 - -1.5$	65	0.471	0.723
	< -1.5	48	0.367	0.755

Table 3: Metallicity-dependent TO colour for dwarf stars along different lines of sight (combined samples).

Direction of line of sight	[Fe/H]	# of stars (in bin)	TO $(b-y)$	TO $(v-y)$
	>0	98	0.431	2.315
Draco 0	$0--0.5$	266	0.397	0.993
+ Draco B	$-0.5--1.0$	215	0.365	0.845
	$-1.0--1.5$	84	0.361	0.819
	<-1.5	68	0.372	0.663
	>0	235	0.431	2.315
Draco 0	$0--0.5$	525	0.394	0.992
+ Draco B	$-0.5--1.0$	452	0.355	0.835
+ Sextans	$-1.0--1.5$	204	0.351	0.809
$(15.0 < y < 20.0)$	<-1.5	178	0.304	0.668
	>0	152	0.899	2.267
	$0--0.5$	454	0.355	0.860
Hercules	$-0.5--1.0$	519	0.338	0.782
$(15.0 < y < 20.0)$	$-1.0--1.5$	280	0.320	0.708
	<-1.5	279	0.287	0.622

Table 4: Turn-off colour for dwarf star populations along different lines of sight.

Direction of line of sight	# of stars (in bin)	TO $(b-y)$	TO $(v-y)$
Draco 0 + Draco B	733	0.361	0.823
Draco 0	379	0.362	0.833
Draco B	354	0.361	0.819
Hercules	599	0.331	0.744
Sextans	233	0.345	0.828
Ursa Major II	239	0.431	0.773

Table 5: Distance-dependent TO colour for dwarf stars along different lines of sight.

Direction of line of sight	Distance from Sun (pc)	# of stars (in bin)	TO $(b-y)$	TO $(v-y)$
	$0-200$	342	0.379	2.262
	$200-400$	194	0.365	0.845
Draco	$400-600$	100	0.356	0.812
	$600-800$	46	0.371	0.839
	$800-1000$	14	0.346	0.785
	>1000	37	0.462	0.663
	$0-200$	472	0.359	2.262
	$200-400$	259	0.365	0.825
Draco	$400-600$	121	0.345	0.818
+ Sextans	$600-800$	53	0.361	0.839
	$800-1000$	15	0.436	0.762
	>1000	17	0.442	0.663
	$0-200$	313	0.348	0.810
	$200-400$	182	0.342	0.781
Hercules	$400-600$	58	0.324	0.684
	$600-800$	21	0.301	0.634
	$800-1000$	8	0.311	0.678
	>1000	17	0.424	0.853

Table 6: TO colour for dwarf stars along different lines of sight, as a function of height above the Galactic plane. Also stars within magnitude range $18.5 < y < 20.0$ are included.

Direction of line of sight	z (pc)	# of stars (in bin)	TO $(b-y)$	TO $(v-y)$
	$0-100$	692	0.525	2.265
	$100-200$	407	0.365	0.825
	$200-300$	203	0.351	0.809
	$300-400$	113	0.375	0.842
Draco	$400-500$	60	0.301	0.839
+ Sextans	$500-600$	31	0.341	0.725
	$600-700$	19	0.398	0.703
	$700-800$	20	0.442	1.003
	$800-900$	12	0.455	0.988
	$900-1000$	6	0.325	0.778
	>1000	34	0.404	0.932
	$0-100$	651	0.345	0.813
	$100-200$	468	0.345	0.779
	$200-300$	250	0.321	0.724
	$300-400$	118	0.301	0.644
	$400-500$	72	0.314	0.672
Hercules	$500-600$	30	0.287	0.635
	$600-700$	28	0.300	0.635
	$700-800$	15	0.327	0.752
	$800-900$	13	0.304	0.663
	$900-1000$	10	0.309	0.650
	>1000	30	0.410	0.812